The EMBO Journal Vol.18 No.7 pp.1738–1747, 1999

A new crystal structure, Ca^{2+} dependence and mutational analysis reveal molecular details of E-cadherin homoassociation

Olivier Pertz, Damir Bozic[1], Alexander W.Koch[2], Charlotte Fauser, Andrea Brancaccio[3] and Jurgen Engel[4]

Department of Biophysical Chemistry, Biozentrum, University of Basel, Klingelbergstrasse 70, 4056 Basel, Switzerland

[1]Present address: Biochemisches Institut, Universitat Zurich, Winterthurer Strasse 190, 8057 Zurich, Switzerland
[2]Present address: Department of Biochemistry and Molecular Biology, Mount Sinai School of Medicine, 1 Gustave L. Levy Place, NY 10029, USA
[3]Present address: Centro di Studio della Chimica dei Recettori e delle Molecole Biologicamente Attive, CNR, Rome, Italy

[4]Corresponding author
e-mail: Engel@ubaclu.unibas.ch

Electron microscopy of ECADCOMP, a recombinant E-cadherin ectodomain pentamerized by the assembly domain of cartilage oligomeric matrix protein, has been used to analyze the role of *cis*-dimerization and *trans*-interaction in the homophilic association of this cell adhesion molecule. The Ca^{2+} dependency of both interactions was investigated. Low Ca^{2+} concentrations (50 μM) stabilized the rod-like structure of E-cadherin. At medium Ca^{2+} concentration (500 μM), two adjacent ectodomains in a pentamer formed *cis*-dimers. At high Ca^{2+} concentration (>1 mM), two *cis*-dimers from different pentamers formed a *trans*-interaction. The X-ray structure of an N-terminal domain pair of E-cadherin revealed two molecules per asymmetric unit in an intertwisted X-shaped arrangement with closest contacts in the Ca^{2+}-binding region between domains 1 and 2. Contrary to previous data, Trp2 was docked in the hydrophobic cavity of its own molecule, and was therefore not involved in *cis*-dimerization of two molecules. This was supported further by W2A and A80I (a residue involved in the hydrophobic cavity surrounding Trp2) mutations in ECADCOMP which both led to abrogation of the *trans*- but not the *cis*-interaction. Structural and biochemical data suggest a link between Ca^{2+} binding in the millimolar range and Trp2 docking, both events being essential for the *trans*-association.

Keywords: cell adhesion/E-cadherin/electron microscopy/mechanism/X-ray crystallography

Introduction

E-cadherin, a 120 kDa transmembrane glycoprotein, belongs to the family of classical cadherins (Ranscht, 1994). Molecules of this family exhibit calcium-dependent homophilic interactions and are involved in selective cell–cell recognition and adhesion (Takeichi, 1990). Therefore, they are important for processes such as embryonic morphogenesis, as well as initiation and maintenance of tissue architecture (Takeichi, 1991; Gumbiner, 1996).

Classical cadherins have a modular structure consisting of five extracellular domains of ~110 amino acids each with internal sequence homology and conserved Ca^{2+}-binding motifs, a transmembrane region and a highly conserved cytoplasmic domain which interacts with actin filaments via catenins (Kemler and Ozawa, 1989; Aberle *et al*., 1996). This link between cadherins and the cytoskeleton allows clustering of cadherins in adherens junctions, a process fundamental for their adhesive function (McNeill *et al*., 1993; Yap *et al*., 1997).

Clustering of cadherins is in the ECADCOMP system (Tomschy *et al*., 1996), in which the E-cadherin ectodomain is fused recombinantly to the coiled-coil assembly domain of cartilage oligomeric matrix protein (COMP) (Efimov *et al*., 1994; Malashkevich *et al*., 1996). This artificially clustered and soluble E-cadherin is able to self-associate, whereas the ectodomain alone is not. This construct therefore provides an *in vitro* model for studying homophilic E-cadherin interactions at the molecular level. Electron microscopy (EM) revealed that in the presence of 2 mM Ca^{2+}, a large fraction of the E-cadherin arms in pentameric ECADCOMP show ring-like structures by interaction of their N-terminal domains to form lateral *cis*-dimers. Two *cis*-dimers from different ECADCOMP molecules can also interact to form 'associated rings'. This 'adhesive *trans*-interaction' represents a second type of homophilic interaction. In addition to 'rings' and 'associated rings', 'star-like' structures were observed in which the cadherin arms did not show any type of interaction.

Ca^{2+} ions are essential for the stabilization of the elongated rod-like structure of E-cadherin (Pokutta *et al*., 1994) and for protection against proteases (Hyafil *et al*., 1981); they are also crucial for the adhesive function (Ozawa *et al*., 1990; Takeichi, 1991). The X-ray structure of the two N-terminal domains of E-cadherin (ECAD12) and N-cadherin (NCAD12) (Nagar *et al*., 1996; Tamura *et al*., 1998) revealed a conserved Ca^{2+}-binding pocket (coordinating the three Ca^{2+} ions with identical ligands and coordination spheres) at the interface between the two domains, and illustrated how the rod-like structure of cadherin is stabilized.

Controversial information about contact regions has emerged from different X-ray structures. Based on crystal lattice contacts observed in the structure of an N-cadherin single domain fragment (NCAD1), Shapiro *et al*. (1995) proposed a two-step association mechanism. First, a *cis*-interaction pair ('strand dimer') is formed between two parallel molecules by mutual exchange of a β-strand due to binding of a tryptophan (Trp2) from one molecule into a hydrophobic pocket of the partner molecule. Secondly, a *cis*-dimerized pair undergoes a *trans*-interaction ('adhesion

dimer') with a complementary antiparallel unit. Alternating *cis*- and *trans*-interactions then form an 'endless' zipper-like superstructure. The same crystal contacts were not observed in the ECAD12 and NCAD12 domain pair structures (Nagar *et al*., 1996; Tamura *et al*., 1998). Here, the closest contact between two parallel aligned molecules was seen in the Ca^{2+}-binding region, and the distance between the two molecules was much too large for the strand exchange as described in the NCAD1 structure. An adhesive *trans*-contact was not observed in the ECAD12 structure, whereas for NCAD12, a different type of adhesion contact was suggested (in contrast to the NCAD1 structure). Furthermore, the zipper model is only in part consistent with the result of Tomschy *et al*. (1996). In the ECADCOMP system, *cis*-dimers were identified as important intermediates, but zipper like superstructures were not observed. Instead, two *cis*-dimers from two different ECADCOMP molecules formed a single *trans*-interaction.

All cadherin X-ray structures showed those molecules to adopt an Ig-like fold (Overduin *et al*., 1995; Shapiro *et al*., 1995; Nagar *et al*., 1996; Tamura *et al*., 1998). The adhesion specificity of the different cadherins resides in the N-terminal domain of the extracellular part (Nose *et al*., 1990). From peptide inhibition studies, the HAV region in domain 1 of E-cadherin (residues 79–81) was proposed to be an adhesion contact region (Blaschuk *et al*., 1990). This adhesion sequence is located on the βCFG surface (Overduin *et al*., 1995; Shapiro *et al*., 1995), but direct evidence for the involvement of this interface in homophilic interactions is still lacking.

The present results demonstrate that, in the ECADCOMP system, lateral *cis*-dimerization occurs at significantly lower Ca^{2+} concentrations than adhesive *trans*-interaction. This *trans*-interaction was found to be abolished by mutation of Trp2, whereas lateral dimerization was not affected. The same result was observed upon mutation of Ala80, which is located in the conserved hydrophobic pocket that binds Trp2. A new crystal structure of ECAD12 was solved in which, in contrast to the earlier structures of domain pairs, all N-terminal residues were clearly defined. In this structure, Trp2 is docked in a hydrophobic pocket of its own molecule and does not bridge between lateral interacting domains.

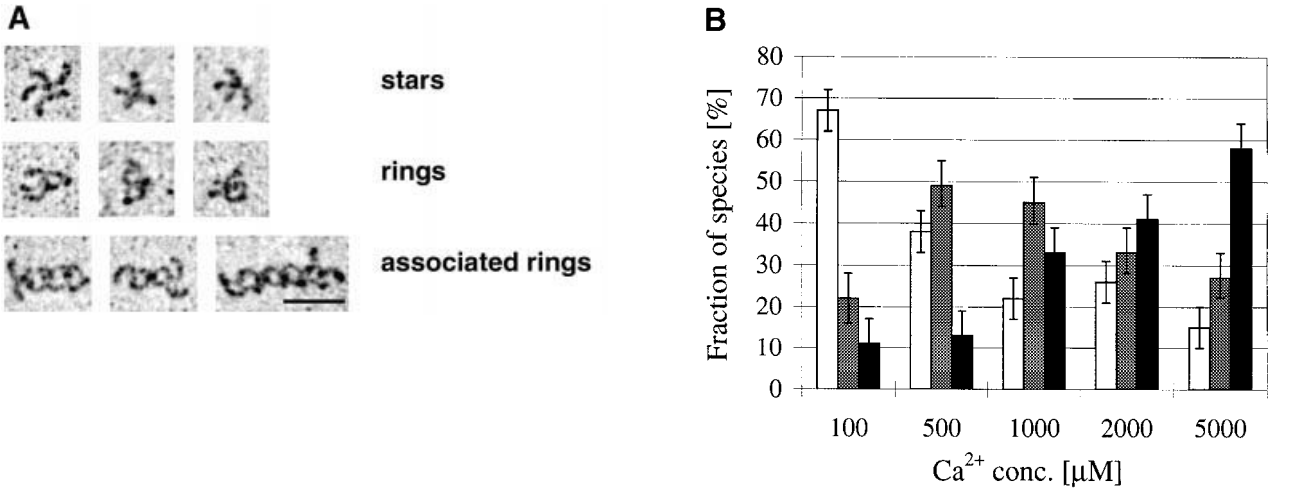

Fig. 1. Different interactions observed in ECADCOMP by electron microscopy after rotary shadowing and their occurrence at different Ca^{2+} concentrations. (**A**) Different species reflecting different interactions observed: 'stars' = pentamers not exhibiting *cis*- nor *trans*-interactions; 'rings' = pentamers which show only *cis*-interactions; 'associated rings' = two or more pentamers involving both *cis*- and *trans*-interactions. The solid bar represents 50 nm. (**B**) Abundance of different species at different Ca^{2+} concentrations: 'stars' (white bars), 'rings' (gray bars) and 'associated rings' (black bars).

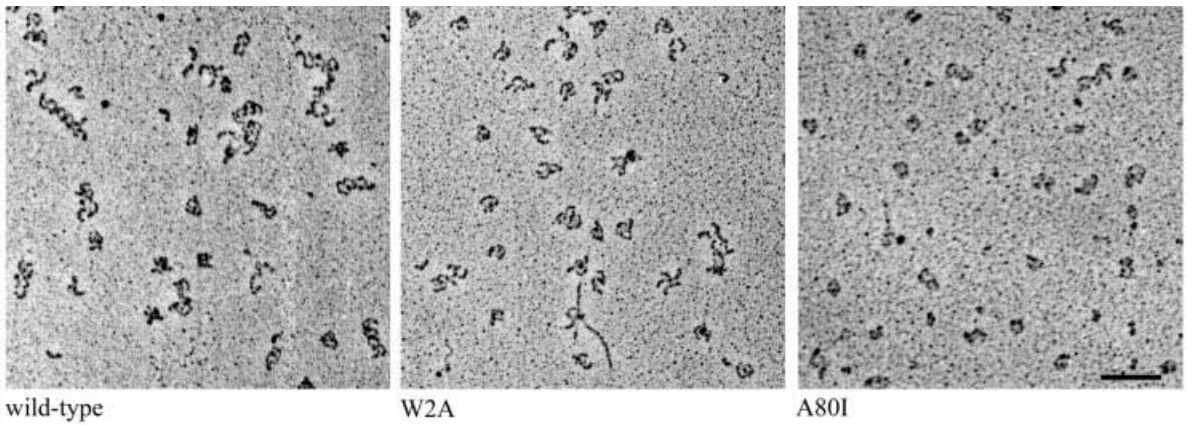

Fig. 2. Electron microscopy of wild-type ECADCOMP, W2A and A80I mutants. Representative fields of rotary-shadowed molecules sprayed at 5 mM [Ca^{2+}] are shown. Wild-type ECADCOMP reveals *cis*- and *trans*-interactions ('associated rings'), whereas both W2A and A80I mutants show only *cis*-interactions (no associated rings). The solid bar represents 100 nm.

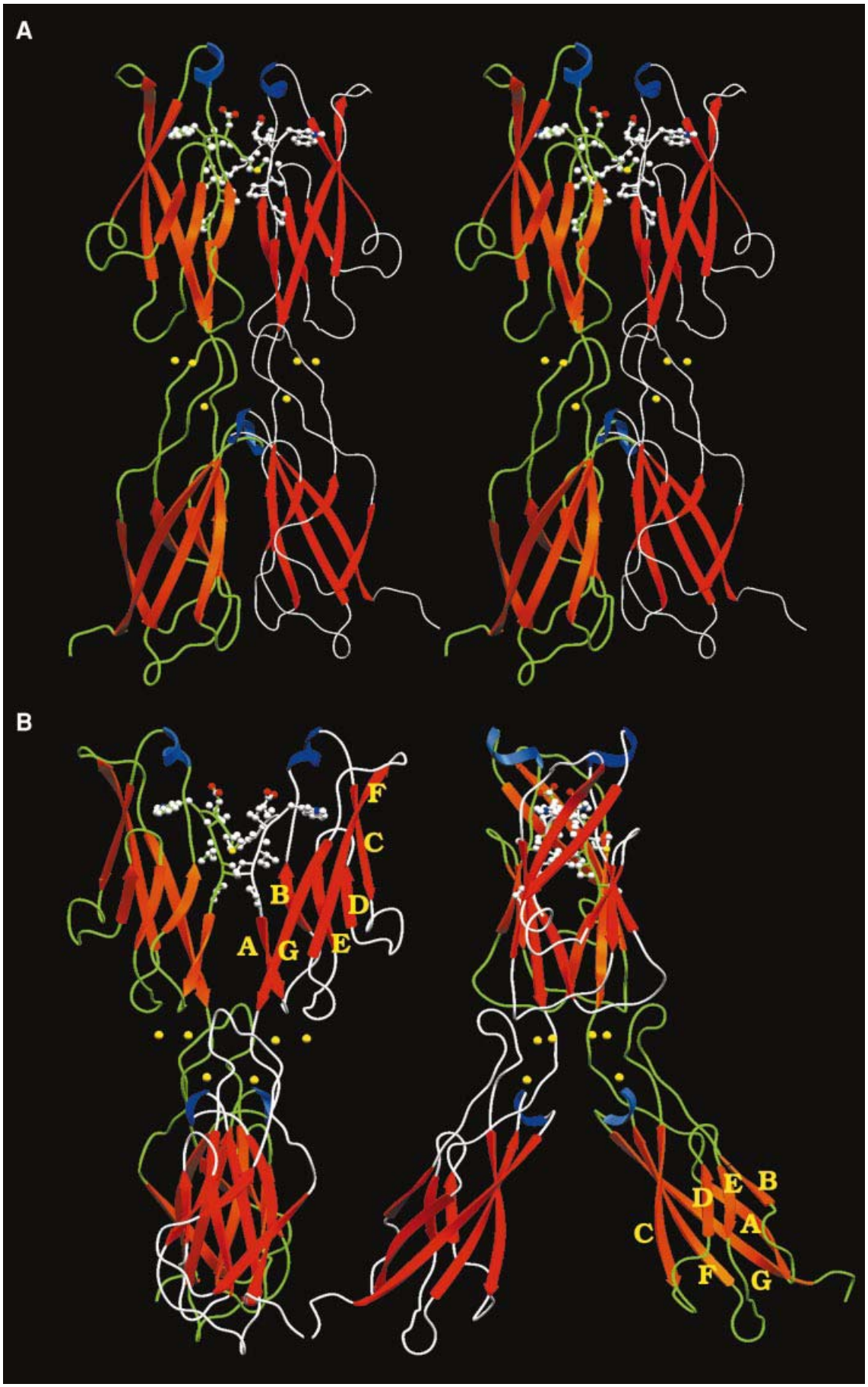
A
B
F
C
B
D
A
G
E
B
E
D
A
C
F
G

Results

Effect of Ca^{2+} on cis- and trans-interactions

We used the ECADCOMP system to dissect the role of Ca^{2+} in the two-step mechanism of cadherin-mediated adhesion. EM of rotary shadowed ECADCOMP molecules was performed at different Ca^{2+} concentrations, in order to determine if one or both types of interaction occurred. For quantification, the fractions of different species (Figure 1A) were determined for >400 molecules at each Ca^{2+} concentration (Figure 1B).

Low Ca^{2+} concentrations (50–100 μM) are sufficient to maintain the rod-like structure of E-cadherin but do not support *cis*- nor *trans*-interactions. Such molecules appear as 'stars' in the EM. Below a Ca^{2+} concentration of 50 μM, the entire structure collapses (not shown), in agreement with earlier observations (Pokutta *et al*., 1994). *Cis*-interactions (ring-like structures) gradually appear at intermediate Ca^{2+} concentrations (500–1000 μM). Finally, above 1 mM Ca^{2+}, *trans*-interactions predominate, giving rise to 'associated rings'. At 5 mM Ca^{2+}, nearly all *cis*-dimers are engaged in *trans*-interactions (Figure 1B).

Abrogation of trans-interactions by mutation of Trp2 and Ala80

In order to evaluate the role of Trp2 in E-cadherin homophilic interactions, two ECADCOMP mutants were designed. Trp2 was mutated to Ala because it has been proposed to participate in *cis*-dimerization by binding to the hydrophobic cavity of a partner molecule in the NCAD1 structure (Shapiro *et al*., 1995). Ala80 was also mutated since its side chain is buried in the hydrophobic cavity to which Trp2 docks. Ala80 was replaced by isoleucine in order to fill this cavity with a larger hydrophobic side chain. This exchange was expected to hinder Trp2 docking due to steric reasons.

For both mutant proteins, electron micrographs revealed

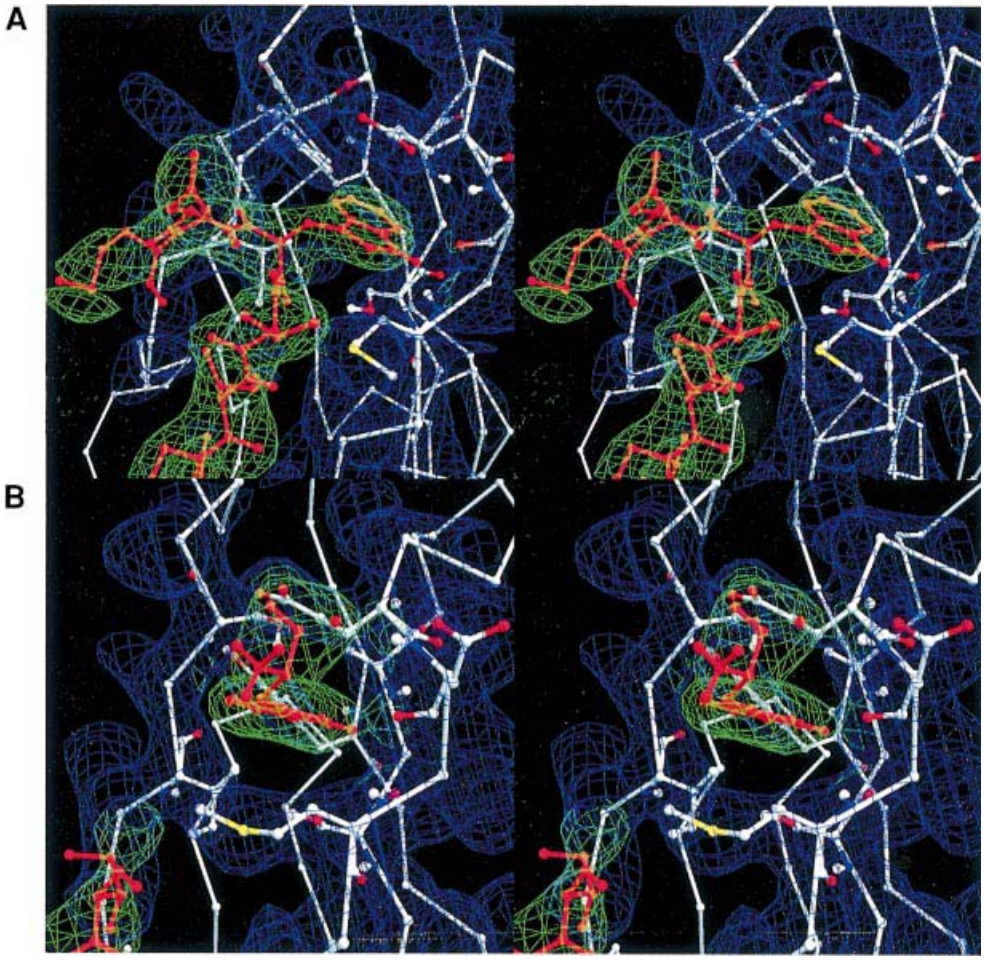

Fig. 4. Final $2F_o–F_c$ stereoplot at a 1σ contour level of a region showing the hydrophobic cavity with (**A**) the βA-strand as in the M-ECAD12 structure and (**B**) the free tryptophan as in the M-ECAD12+W structure. Continuous density (green) is observed for the βA-strand (red), with chain tracing being unambiguous (A), whereas it could only be traced from Ile4 in (B); additional density in the hydrophobic pocket was interpreted as a free tryptophan. The figure was prepared with DINO (Phillipsen, 1998).

Fig. 3. Stereoview of the M-ECAD12 structure (**A**) and two monoviews of the same structure rotated 90° from each other (**B**). Ca^{2+} atoms are represented as yellow spheres, and residues on the βA-strand are shown in a ball and stick representation. Secondary structure is assigned according to DSSP (Kabsch and Sander, 1983) and structure nomenclature is according to Wagner (1995). The previously described, rather unusual β-helix (Nagar *et al*., 1996) resides between the strands βC and βD. Figures were prepared with SETOR (Evans, 1993).

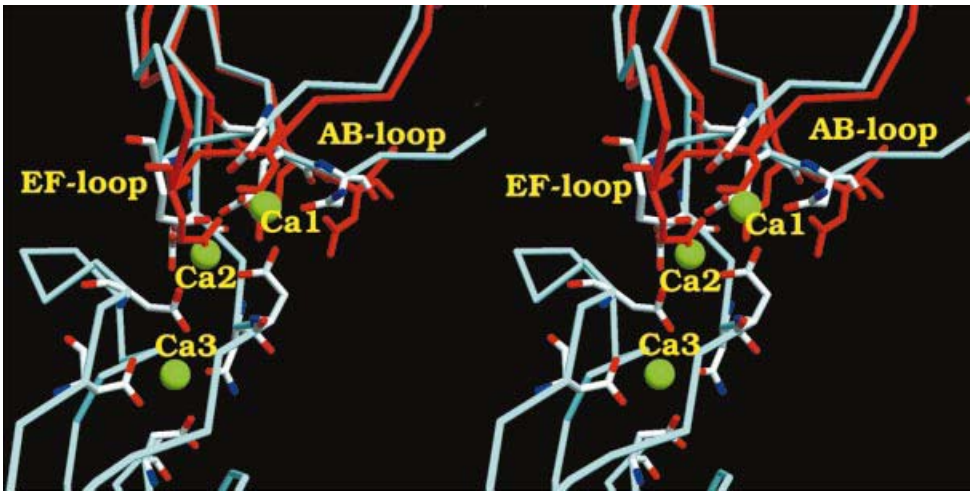

Fig. 5. Stereoview of the Ca^{2+}-binding site of the M-ECAD12 structure (blue) superimposed with the NCAD1 structure (red). The side chains of residues involved in Ca^{2+} coordination are shown and are identical to those found in the previously described MR-ECAD12 structure (Nagar *et al*., 1996), except for one additional coordination of Ca1 by the strictly conserved Asn12 at a distance of 3 Å which replaces the coordination of a tightly bound water molecule. The figure was prepared with DINO (Phillipsen, 1998).

abundant ring-like structures but a total lack of associated rings at 2 (data not shown) and 5 mM Ca^{2+} (Figure 2). This demonstrates that W2A and A80I mutations in ECADCOMP abolish the adhesive *trans*-interaction but that lateral *cis*-interactions still occur. These results are in contradiction with the bridging hypothesis in which Trp2 mediates dimerization between two single domains (Shapiro *et al*., 1995).

The crystal structure of the first two E-cadherin domains

Two different E-cadherin constructs were used for crystallization experiments. One construct comprises the first two E-cadherin domains but contains an additional methionine in front of the native N-terminus (M-ECAD12; Koch *et al*., 1997). This fragment was crystallized and the structure was solved at a resolution of 0.29 nm by Patterson search techniques using the previously solved MR-ECAD12 fragment (Nagar *et al*., 1996) (Protein Data Bank accession code 1EDH) which has Met–Arg as two extra N-terminal residues. An ECAD12 fragment with the native N-terminus was also expressed in *Escherichia coli* but could not be crystallized due to severe aggregation phenomena (analyzed by ultracentrifugation experiments). It was, however, correctly folded as judged by circular dichroism spectroscopy and resistance to trypsin digestion (data not shown). We also evaluated the role of Trp2 by competition binding of free soluble tryptophan (saturating conditions) to the M-ECAD12 fragment. Co-crystals were obtained and the structure was solved at a resolution of 0.28 nm. This complex is designated as M-ECAD12+W.

In both structures, the organization of two domain pairs in the asymmetric unit can be described as an intertwisted X-shaped form with closest contacts in the Ca^{2+}-binding region between the two domains (Figure 3). In the M-ECAD12 structure, Trp2 is docked into the hydrophobic pocket formed by residues of its own molecule (Figures 3 and 4A) and not into that of a neighboring molecule ('strand dimer' observed in the NCAD1 structure). In previous structures of the domain pairs MR-ECAD12 (Nagar *et al*., 1996) and NCAD12 (Tamura *et al*., 1998), Trp2 was not defined and its docking mode was therefore not resolved.

An interesting feature of the M-ECAD12+W structure was its non-symmetric binding of free tryptophan. In one molecule of the asymmetric unit, binding of free tryptophan was observed in the hydrophobic cavity (Figure 4B), and electronic density for the residues Met1-Asp1-Trp2-Val3 of the corresponding βA-strand was not defined, indicating a non-ordered state. In the other molecule, regular docking of Trp2 was observed and the structure was identical to that of M-ECAD12 without tryptophan addition (Figure 4A).

Discussion

Influence of Ca^{2+} ions on cis- and trans-interactions

These results, together with previous observations (Shapiro *et al*., 1995; Nagar *et al*., 1996; Tomschy *et al*., 1996; Yap *et al*., 1997), provide compelling evidence that the process of cadherin-mediated adhesion consists of a parallel, lateral *cis*-interaction and an antiparallel, adhesive *trans*-interaction. By measuring the Ca^{2+} dependence of the two interactions, we were able to dissect the two steps of the adhesion process.

The Ca^{2+} dependence of the *cis*- and *trans*-interactions can be explained by the distinct binding affinities of different sites (Koch *et al*., 1997). The complete extracellular E-cadherin region with its four Ca^{2+}-binding pockets between the five domains binds nine Ca^{2+} ions with an average K_d of 30 μM. The Ca^{2+}-binding pocket at the interface between domains 1 and 2 binds three Ca^{2+} ions, two with K_ds of 330 μM and one with a K_d of 2 mM. Ca1 in the MR-ECAD12 structure (Figure 5) has been proposed to be the low affinity binding site since this Ca^{2+} ion is the only one exposed to the surface (Koch *et al*., 1997). These structural aspects and the calcium-

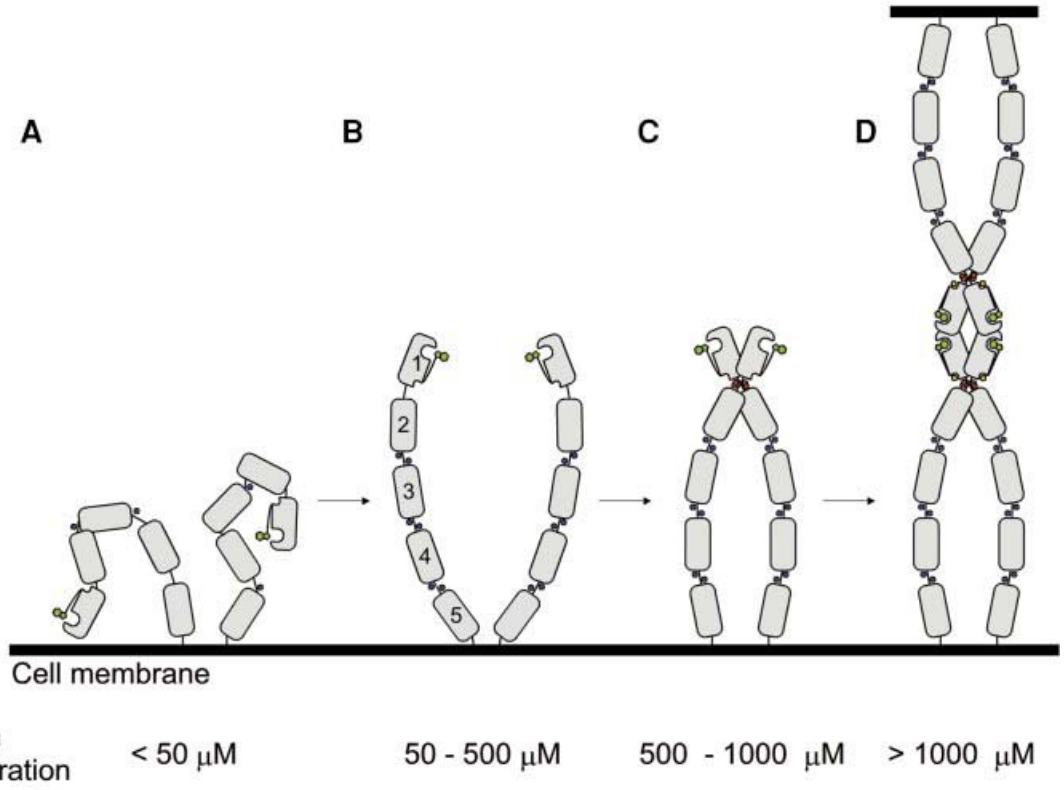

Fig. 6. Proposed scheme of the effect of calcium on membrane-clustered E-cadherin. Low Ca^{2+} concentrations stabilize the rod-like structure (**A** and **B**), medium and high concentrations result in *cis*-dimerization (**C**) and Trp2 docking in its hydrophobic cavity which enables *trans*-interaction (**D**). Domains 1–5 are drawn as gray blocks, with the hydrophobic cavity to which Trp2 binds in domain 1. Trp2 is shown as a green symbol with the βA-strand as a connecting black line. Bound Ca^{2+} ions are symbolized by circles and the different K_d values of the distinct binding sites by different colors: blue, 30 μM; red, 330 μM; yellow, 2 mM.

binding affinities correlate with the EM data in the present report. At 100 μM Ca^{2+}, binding sites at domain junctions 2–3, 3–4 and 4–5 are saturated, but only a few Ca^{2+} ions bind between domains 1 and 2 (Figure 6B). Therefore, the rod-like structure is preserved but only a few *cis*- and even fewer *trans*-interactions occur. At 500 μM Ca^{2+}, at which two of the three binding sites between domains 1 and 2 (with a K_d of 330 μM) are saturated, *cis*-interactions are predominant but only a few *trans*-interactions are seen (Figure 6C). Finally, when Ca^{2+} is increased to 1 mM, *trans*-interactions appear and become more prominent at 2 and 5 mM Ca^{2+}, demonstrating the importance of saturation of the weak binding site for *trans*-interactions (Figure 6D). Remarkably, our data demonstrate that the rod-like structure, which is already supported at rather low Ca^{2+} concentration, seems to be necessary but not sufficient for cadherin-mediated adhesion, and that the role of Ca^{2+} goes far beyond a solely structural one.

The importance of a low affinity Ca^{2+}-binding site for adhesive *trans*-interactions points to a possible physiological regulation of adhesive function by external calcium. Although the free extracellular Ca^{2+} concentration in human blood is regulated stringently to 1.2 mM, there are examples of other extracellular fluids in which this concentration varies by a factor of ~10 (Brown *et al*., 1995; Maurer *et al*., 1996). The relatively high K_d values found for the Ca^{2+}-binding pocket between domains 1 and 2 are within the range of possible Ca^{2+} concentration changes. Electrophysiological *in vivo* studies have shown a Ca^{2+} dependence of the inhibitory effect of HAV peptides on N- and E-cadherin adhesiveness at synaptic sites (Tang *et al*., 1998). These peptides have been shown to interfere with many different cadherin-dependent processes, including neutrite outgrowth (Chuah *et al*., 1991; Doherty *et al*., 1991), osteoblastic formation (Mbalaviele *et al*., 1995) and myoblast fusion (Mege *et al*., 1992). Tang *et al*. (1998) clearly demonstrated that a transient depletion of Ca^{2+} in the synaptic cleft, due to the flux through voltage-gated Ca^{2+} channels, caused the adhesive properties of cadherins to become sensitive to HAV peptides and blocking antibodies, whereas the effect was not present when the Ca^{2+} concentration was kept at 5 mM. These experiments strongly support the notion of a direct influence of extracellular Ca^{2+} concentration changes on cadherin-mediated cell adhesion.

Cis-dimerization site

In the asymmetric units of their crystal structure, domain pairs M-ECAD12 (Figure 3) and MR-ECAD12 (Nagar *et al*., 1996) both appear as an intertwisted X-shaped dimer, with the most intimate contacts at the Ca^{2+}-binding regions. The NCAD12 structure (Tamura *et al*., 1998) shows a single molecule in the asymmetric unit, but a similar contact can be seen between symmetric equivalent molecules in the crystal. In this case, a wider angle between the two molecules is observed compared with M-ECAD12 and MR-ECAD12 (D.Bozic, personal communication). In solution, both M-ECAD12 and MR-ECAD12 dimerize in a Ca^{2+}-dependent manner, which is consistent with the Ca^{2+} dependence of *cis*-dimerization

in ECADCOMP. Relatively high values for a dissociation constant, K_d = 0.1 mM for M-ECAD12 and K_d = 0.2 mM for MR-ECAD12 (Alattia *et al*., 1997; Koch *et al*., 1997), indicate a weak protein–protein interaction and suggest the existence of a dimer in a crystallization solution or in ECADCOMP, in which the local concentration of ectodomains is estimated to be 0.1–2 mM (Tomschy *et al*., 1996).

Crystal contacts are first of all determined by crystal forces and therefore do not necessarily represent biological relevant interaction sites. From the orientation of the molecules in the domain pair structures, it seems unlikely that Trp2 is responsible for *cis*-interactions via strand exchange as observed in the NCAD1 structure. This is supported further by the W2A and A80I mutations in ECADCOMP which do not affect *cis*-dimerization. The Ca^{2+} dependency of the *cis*-interaction as observed in the ECADCOMP system supports the notion that the Ca^{2+}-binding site between domains 1 and 2 may be the *cis*-dimerization site, but direct proof that this interaction is also present in solution is still lacking.

Trp2 docks into a hydrophobic cavity of its own molecule enabling trans-interactions

Based on the new E-cadherin structures solved in the present work (M-ECAD12 and M-ECAD12+W), it is possible to re-evaluate the role of Trp2 on a molecular level. In contrast to all other solved structures of domain pairs (Nagar *et al*., 1996; Tamura *et al*., 1998), the N-terminal residues including Trp2 are well defined in our structure. These differences may be sought in the crystallization conditions and/or in the number and type of extraneous N-terminal residues. Incomplete removal of the E-cadherin propeptide is known to abolish adhesive activity (Ozawa and Kemler, 1990). The additional arginine in MR-ECAD12 turned out to be the last residue of the propeptide and may explain the absence of an ordered N-terminus in the MR-ECAD12 structure. The high structural definition of the fragment M-ECAD12 clearly reveals binding of Trp2 into a hydrophobic pocket formed by residues of its own polypeptide chain (Figures 3A and 4A) and not into the identical pocket of an adjacent molecule as was observed in the crystal structure of the single domain fragment NCAD1 (Shapiro *et al*., 1995).

Our mutational data indicate that Trp2 and the conserved hydrophobic pocket are essential for the *trans*-interaction. Mutation of Trp2 to alanine or Ala80 to isoleucine (which blocks the pocket for tryptophan docking) led to a complete loss of *trans*-interactions without affecting *cis*-dimerization in ECADCOMP (Figure 2). Dissection of the two interactions could not be reached with cell aggregation assays (Tamura *et al*., 1998), but the loss of cell adhesion with similar mutants is in complete agreement with our data. Tamura *et al.* (1998) used indole-3-acetic acid, a tryptophan analog, as a competitive inhibitor which could bind to the hydrophobic cavity, and observed a 60% inhibition of cell adhesion after addition of this substance. Similar results with soluble tryptophan as a competitive inhibitor using the ECADCOMP system indicated that the inhibition is based on prevention of the *trans*-interaction without any effect on *cis*-dimerization (data not shown).

The M-ECAD12+W structure showed that free soluble tryptophan can bind into the hydrophobic cavity, resulting in a non-ordered state of the corresponding βA-strand. This happened in only one of the two molecules in the asymmetric unit, whereas regular Trp2 docking, as in the M-ECAD12 structure, was observed in the other molecule. The reason for this non-symmetric behavior may be sought in crystal forces or a nucleation phenomenon during crystal formation. This structural information suggests that two different conformations exist and are related to two different functional states: (i) the βA-strand is labile and Trp2 is not docked in its hydrophobic cavity, as observed in the M-ECAD12+W structure; and (ii) the βA-strand is rigid, allowing Trp2 docking, as observed in the M-ECAD12 structure, and enabling *trans*-interaction. It may be speculated that conformational changes upon removal of the propeptide (Ozawa and Kemler, 1990) can be readily transmitted to the docking state of the nearby Trp2. The requirement for high Ca^{2+} concentrations for the *trans*-interaction may be explained by a link between Ca^{2+} binding and Trp2 docking. This link might be provided by Glu11 and Asn12 located on the AB-loop (for definitions see Figure 3B) which are part of the proposed low affinity Ca^{2+}-binding site (Ca1 in Figure 5) that has to be saturated for adhesive function and that is directly adjacent to the βA-strand. We therefore propose a mechanism in which Ca^{2+} binding to the low affinity site helps to stabilize the βA-strand, which in turn facilitates Trp2 docking to the hydrophobic cavity. This docking process could induce a conformational change in the backbone of the hydrophobic pocket formed by the βCFG sheet. Interestingly, this is also believed to be the adhesive interface (Nose *et al*., 1990; Overduin *et al*., 1995; Shapiro *et al*., 1995).

The docking of Trp2 into the hydrophobic cavity of an adjacent molecule observed in the NCAD1 structure (Shapiro *et al*., 1995) may be explained by the lack of a second domain in this fragment which results in an incomplete Ca^{2+}-binding pocket. Superposition of the structures of NCAD1 and the first domain of M-ECAD12 (Figure 5) shows that the most pronounced structural differences reside in the AB/EF-loop regions where Glu11 and Asn12 (AB-loop) contribute to the proposed low affinity Ca1-binding site. The lack of Ca^{2+} coordination may increase the motional freedom of the adjacent βA-strand, preventing docking of Trp2 into its own hydrophobic cavity. The relative lability of the βA-strand may explain the possibility of a strand exchange dimerization, as observed in the NCAD1 structure, and the ability of this fragment to dimerize in a Ca^{2+}-independent manner in solution (Shapiro *et al*., 1995).

Conclusions and outlook

The present results strengthen the idea that lateral *cis*-dimerization of cadherin molecules is a prerequisite for adhesive activity (Tomschy *et al*., 1996; Yap *et al*., 1997, 1998; Norvell and Green, 1998). Very recently, *in vivo* active dimers *in cis* configuration were also identified as active precursors by chemical cross-linking studies (Takeda *et al*., 1999). Interestingly, *cis*-dimerization is not sufficient for cadherin *trans*-association, and a second determinant, a Ca^{2+} concentration in the millimolar range, is also required for the adhesive activity. This raises an attractive possibility for regulation of cell adhesion on the extracellular side. Our data also re-evaluate the role of

Table I. Data collection statistics

Data set	Observed reflections	Independent reflections	Maximal resolution	Completeness	Completeness (last shell)	R_{merge}[a]
M-ECAD21	2852	13 451	0.293 nm	95.5%	81.5% (0.300–0.293 nm)	13.8%
M-ECAD12+W	31 431	15 393	0.277 nm	94.5%	74.4% (0.284–0.277 nm)	9.2%

[a]$R_{merge} = \Sigma_h \Sigma_i |I_i(h) - <I(h)>| / \Sigma_h \Sigma_i I_i(h)$, where $I_i(h)$ is the intensity value of the ith measurement of h and $<I(h)>$ is the corresponding value h for all i measurements of h; the summation is over all measurements.

Table II. Refinement statistics of the M-ECAD12 and M-ECAD12+W structures

	M-ECAD12		M-ECAD12+W	
	No. of atoms	Average *B*	No. of atoms	Average *B*
Protein				
Main chain	1752	27.6	1753	34.7
Side chain	1608	32.3	1603	38.0
All atoms	3360	29.8	3357	36.3
Water	266	35.3	382	44.1
Ca^{2+}	6	15.1	6	16.6
All atoms	3632	30.12	3745	37.0
R.m.s.d. bonds	0.0010 nm		0.0006 nm	
R.m.s.d. angles	1.64		1.51	
R-factor	19.86 (1.000–0.293 nm)		20.34 (3.3–0.28 nm)	
Ramachandran plot				
Most favored	84.8%		85.9 %	
Additionally allowed	15.8%		13.8%	
Generously allowed	0.0%		0.0%	
Not allowed	0.0%		0.3%[a]	

[a]Trp2 is backbone hydrogen bonded to βB strand residue Lys25 O. In the M-ECAD12 structures, both Trp2 residues are in the additionally allowed region.

the conserved Trp2 and suggest how Ca^{2+} may trigger the adhesive function on a molecular level. A possible scheme for the mechanism is shown in Figure 6. Two major questions remain, the identification of a region involved in *trans*-interaction, and the determinants of cadherin specificity.

Materials and methods

DNA constructions

PCR followed standard protocols with *Pfu* polymerase (Stratagene). *Escherichia coli* DH10b was used as cloning host strain. Amplified products were sequenced with a T7 sequencing kit (Pharmacia).

The overlap extension method (Ho, 1990) was used to insert a silent mutation which permits addition of a *Bfr*I restriction site in the coding sequence of the ECADCOMP construct, a *Kpn*I site at its 5′ end and an *Xba*I site at its 3′ end. In a first round of PCR, pECAD-COMP (Tomschy *et al*., 1996) as template and the following sets of primers were used: 5′-ACTATAGGGAGGTACCGCTAGCATGGGAGCCC-3′ (primer 1) and 5′-GGCTGTTGTGCTCAAGCCTTCGCCT-3′, and 5′-AGGCGAA-GGCTTGAGCACAACAGCC-3′ and 5′-ACACTATAGAATAGGGC-CCTCTAGA-3′ (primer 2). The two resulting fragments were gel purified using the QIAquick gel extraction kit (Qiagen) and mixed with primers 1 and 2 for a second amplification. The amplified product was then digested and cloned into pBluescript KS (Stratagene) using *Kpn*I and *Xba*I sites, and resulting in the plasmid pBSECADCOMP.

The megaprimer method (Gobinda and Sommer, 1990) was used to generate single point mutations. In a first round of PCR, pBSECAD-COMP as a template and the primer sets: 5′-ACGAGACGCGGTCATC-CCTC-3′ and 5′-GGGGGGTTTGTCAGCTCCTT-3′, and 5′-CTC-CCATCAGCTGCCCCG-3′ and 5′-TGATGACACAATATGAGAAT-3′ were used to generate the W2A and A80I megaprimers. These were then purified with a QIAquick PCR extraction kit (Qiagen) and used in a second round of amplification with the same template. A fragment resulting from amplification with W2A megaprimer and primer 1 was digested, gel purified and cloned into pBSECADCOMP using *Kpn*I and *Eco*RI sites. The same procedure was done with A80I megaprimer and 5′-GGGGGCATCATCATCGGT-3′, and cloning was achieved using *Eco*RI and *Bfr*I sites. Mutations were checked by sequencing. The mutant fragments in pBSECADCOMP were then digested by *Kpn*I and *Xba*I and cloned into the expression vector pCEP4 (InVitrogen) using *Kpn*I and *Nhe*I sites, resulting in the pCEP4ECADCOMP vectors.

Cell culture, transfection and expression of ECADCOMP mutants

Human embryonal kidney 293 EBNA cells (Invitrogen) were cultured in Dulbecco's modified Eagle's medium (DMEM) F12 supplemented with 10% fetal calf serum (FCS), 1% glutamine and 10 μg/ml PenStrep. All reagents were purchased from Gibco-BRL. Transfection was carried out on a large scale by the calcium phosphate method. Cells were plated in 500 ml flasks (Falcon) and were grown until 80% confluency. At 4 h before transfection, the medium was switched to 28 ml of DMEM, 10% FCS, 1% glutamine per flask. Then 5 μg of a pCEPECADCOMP mutant was mixed with 50 μg of carrier DNA, and water was added to 0.7 ml. To this mixture, 0.7 ml of 0.5 M $CaCl_2$, 0.1 M HEPES pH 7.0 was added for a 10 min incubation, then 1.4 ml of 0.75 mM Na_2HPO_4, 0.75 mM NaH_2PO, 0.05 M HEPES pH 7.0, 0.28 M NaCl was added for a second 10 min incubation. The whole mix was then given to the cells overnight. The next day, the cells were washed twice with TBS (25 mM Tris–HCl pH 7.4, 137 mM NaCl, 5 mM KCl, 0.7 mM $CaCl_2$, 0.5 mM $MgCl_2$) and switched to 17 ml of expression medium (DMEM F12, 1% glutamine, 10 μg/ml PenStrep) per flask. After 2 days of expression, conditioned medium was collected and new expression medium was added. This procedure was repeated 10–12 times. Supernatant was centrifuged at 2500 *g* for 10 min and stored at –20°C.

The isolation of the recombinant protein was performed as described previously (Tomschy *et al.*, 1996).

Electron microscopy

Fresh protein preparations of ECADCOMP and of mutated ECADCOMP (W2A, A80I) were used at a protein concentration of 0.05–0.1 mg/ml in 20 mM Tris–HCl, pH 7.4 containing 2 or 5 mM $CaCl_2$. For electron microscopy at different Ca^{2+} concentrations, samples were Ca^{2+} depleted with EDTA, dialyzed against Ca^{2+}-free buffer and, finally, against Ca^{2+}-containing buffers. Each sample was diluted 1:1 (v/v) with 80% glycerol containing the same Ca^{2+} concentration and sprayed onto freshly cleaved mica. Rotary shadowing was performed with platinum/carbon at an angle of 9° and carbon shadowing at an angle of 90°. Replica formation and electron microscopy were performed as described elsewhere (Engel, 1994). For statistical evaluations, the different species of ECADCOMP ('stars', 'rings' and 'associated rings') were counted on electron micrographs. For each calcium concentration, 6–8 fields were evaluated, resulting in a total of 400–1000 molecules. The standard deviation was calculated by comparing different fields.

Crystallization of the M-ECAD12 fragment, data collection and evaluation

The M-ECAD12 fragment was prepared as described by Koch *et al.* (1997). Crystals were grown by mixing equivalent amounts of the protein (7.5 mg/ml in 20 mM Tris–HCl pH 7.4, 150 mM NaCl, 2 mM $CaCl_2$) with precipitant (50 mM ammonium sulfate, 50 mM NaOAc, 30% PEG 8000, pH 8.5 Tris–HCl) and equilibrating this mixture against 500 µl of the precipitant solution using the hanging drop vapor diffusion method. In the case of co-crystallization with free soluble tryptophan, protein was first dialyzed against saturating amounts of tryptophan. The precipitant solution (100 mM ammonium sulfate, 100 mM NaOAc, 25% PEG 8000 at pH 8.0 Tris–HCl) was then used as mentioned above.

In both cases, platelet-shaped crystals grew after 2 weeks at room temperature to suitable measurement size in the space group C2, having the almost isomorphous cell constants a = 12.250 nm, b = 8.056 nm, c = 7.344 nm, $\alpha = \gamma = 90°$ and β = 113.98°, and a = 12.057 nm, b = 8.064 nm, c = 7.280 nm, $\alpha = \gamma = 90°$ and β = 112.84°, respectively. Both crystal forms contain two molecules in the asymmetric unit and have a solvent content of 58%.

All data were collected at room temperature on a MARResearch™ image plate scanner mounted on an Elliot GX20 rotating anode generator operating at the wavelength λ = CuKα = 1.5418 Å. The X-ray intensities were evaluated with the MOSFLM package (Leslie, 1990); data scaling and reduction were performed within the CCP4 package (Collaborative Computational Project, number 4, 1994). A summary of data collection statistics is given in Table I.

The data sets were submitted to a molecular replacement calculation using the program AMoRe (Navaza, 1994) with the coordinates of one molecule of the previously solved MR-ECAD12 fragment (Protein Data Bank accession code 1EDH). In both cases, two unambiguous solutions were found. The data sets were submitted to a first simulated annealing run with X-PLOR (Brunger, 1992) using non-crystallographic symmetry (NCS) restrains. The resulting densities were then averaged interactively with the program MAIN (Turk, 1988), and regions where the averaged densities disappeared or got worse were taken out of the NCS restrains in further refinements (residues 1–5, 25–35, 81–93 and 210–218). The structure was rebuilt consecutively and refined with X-PLOR using the parameters derived by Engh and Huber (1991). The final crystallographic *R*-factors are 19.8% (M-ECAD12) and 20.3% (M-ECAD12+W). The refinement statistics are summarized in Table II.

At the final stages of the refinement of the M-ECAD12+W structure, additional and continuous density branching at Cys9 was observed, indicating two distinct conformeric states of the N-termini for both molecules in the asymmetric unit. Three and two additional amino acids could be traced in unambiguously as minor occupied alternative conformations of the N-terminus. The correctness of the observation was proven by simulated annealing omit maps and the decrease of the free *R*-factor upon inclusion of each of the two and both alternative conformers. As prior to this observation the free *R*-factor was not included in the refinement protocol, as the structures contained none, each one and both additional conformers were submitted to a full simulated annealing run. Upon inclusion of the first and second conformer, the free *R*-factor dropped 0.7% and an additional 0.3%, respectively. The occupancies of each of the four alternate states were set to 0.5. Except for this procedure, the free *R*-factor was not used in previous and further refinement.

Acknowledgements

We are grateful to Dr Ulrike Mayer and Dr Andrea Tomschy for fruitful discussions, and to Professor Charles David for assistance with writing the manuscript. This work was supported by the EU program Biotechnology II, the Swiss Bundesamt fur Wissenschaft und Forschung and a grant from the Swiss Science Foundation.

References

Aberle,H., Schwartz,H. and Kemler,R. (1996) Cadherin–catenin complex: protein interactions and their implications for cadherin function. *J. Cell. Biochem.*, **61**, 514–523.

Alattia,J.R., Ames,J.B., Porumb,T., Tong,K.I., Heng,Y.M., Ottensmeyer,P., Kay,C.M. and Ikura,M. (1997) Lateral self-assembly of E-cadherin directed by cooperative calcium binding. *FEBS Lett.*, **417**, 405–408.

Blaschuk,O.W., Sullivan,R., David,S. and Pouliot,Y. (1990) Identification of a cadherin cell adhesion recognition sequence. *Dev. Biol.*, **139**, 227–229.

Brown,E.M., Vassilev,P.M. and Hebert,S.C. (1995) Calcium ions as extracellular messengers. *Cell*, **83**, 679–682.

Brunger,A.T. (1992) *X-PLOR, Version 3.1: A System for X-ray Crystallography and NMR*. Yale University Press, New Haven, CT.

Chuah,M.I., David,S. and Blaschuk,O. (1991) Differentiation and survival of rat olfactory epithelial neurons in dissociated cell culture. *Brain Res. Dev. Brain Res.*, **60**, 123–132.

Collaborative Computational Project No. 4 (1994) The CCP4 suite: programs for protein crystallography. *Acta Crystallogr.*, **D50**, 760–763.

Doherty,P., Rowett,L.H., Moore,S.E., Mann,D.A. and Walsh,F.S. (1991) Neurite outgrowth in response to transfected N-CAM and N-cadherin reveals fundamental differences in neuronal responsiveness to CAMs. *Neuron*, **6**, 247–258.

Efimov,V.P., Lustig,A. and Engel,J. (1994) The thrombospondin-like chains of cartilage oligomeric matrix protein are assembled by a five-stranded α-helical bundle between residues 20 and 83. *FEBS Lett.*, **341**, 54–58.

Engel,J. (1994) Electron microscopy of extracellular matrix components. *Methods Enzymol.*, **245**, 469–488.

Engh,R.A. and Huber,R. (1991) Accurate bond and angle parameters for X-ray protein structure refinement. *Acta Crystallog. sect. A*, **47**, 392–400.

Evans,S.V. (1993) SETOR: Harvard-lighted three dimensional solid model representation of macromolecules. *J. Mol. Graph.*, **11**, 134–142.

Gobinda,S. and Sommer,S.S. (1990) The megaprimer method of site directed mutagenesis. *BioTechniques*, **8**, 404–407.

Gumbiner,B.M. (1996) Cell adhesion: the molecular basis of tissue architecture and morphogenesis. *Cell*, **84**, 345–357.

Ho,S. (1990) Site directed mutagenesis and gene splicing by overlap extension. *DNA Protein Eng.*, **2**, 50–55.

Hyafil,F., Babinet,C. and Jacob,F. (1981) Cell–cell interactions in early embryogenesis: a molecular approach to the role of calcium. *Cell*, **26**, 447–454.

Kabsch,W. and Sander,C. (1983) Dictionary of secondary structures: pattern recognition of hydrogen-bonded and geometrical features. *Biopolymers*, **22**, 2577–2637.

Kemler,R. and Ozawa,M. (1989) Uvomorulin–catenin complex: cytoplasmic anchorage of a Ca^{2+}-dependent cell adhesion molecule. *BioEssays*, **11**, 88–91.

Koch,A.W., Pokutta,S., Lustig,A. and Engel,J. (1997) Calcium binding and homoassociation of E-cadherin domains. *Biochemistry*, **36**, 7697–7705.

Leslie,A.G.W. (1990) *Crystallographic Computing*. Oxford University Press, New York, NY.

Malashkevich,V.N., Kammerer,R.A., Efimov,V.P., Schulthess,T. and Engel,J. (1996) The crystal structure of a five-stranded coiled coil in COMP: a prototype ion channel? *Science*, **274**, 761–765.

Maurer,P., Hohenester,E. and Engel,J. (1996) Extracellular calcium-binding proteins. *Curr. Opin. Cell Biol.*, **8**, 609–617.

Mbalaviele,G., Chen,H., Boyce,B.F., Mundy,G.R. and Yoneda,T. (1995) The role of cadherin in the generation of multinucleated osteoclasts from mononuclear precursors in murine marrow. *J. Clin. Invest.*, **95**, 2757–2765.

McNeill,H., Ryan,T.A., Smith,S.J. and Nelson,W.J. (1993) Spatial and temporal dissection of immediate and early events following cadherin-mediated epithelial cell adhesion. *J. Cell Biol.*, **120**, 1217–1226.

Mege,R.M., Goudou,D., Diaz,C., Nicolet,M., Garcia,L., Geraud,G. and Rieger,F. (1992) N-cadherin and N-CAM in myoblast fusion: compared localisation and effect of blockade by peptides and antibodies. *J. Cell Sci.*, **103**, 897–906.

Nagar,B., Overduin,M., Ikura,M. and Rini,J.M. (1996) Structural basis of calcium-induced E-cadherin rigidification and dimerization. *Nature*, **380**, 360–354.
Navaza,J. (1994) AMORE: an automated procedure for molecular replacement. *Acta Crystallogr.*, **A50**, 157–163.
Norvell,S. and Green,K. (1998) Contributions of extracellular and intracellular domains of full length and chimeric cadherin molecules to junction assembly in epithelial cells. *J. Cell Sci.*, **111**, 1305–1318.
Nose,A., Tsuji,K. and Takeichi,M. (1990) Localization of specificity determining sites in cadherin cell adhesion molecules. *Cell*, **61**, 147–155.
Overduin,M., Harvey,T.S., Bagby,S., Tong,K.I., Yau,P., Takeichi,M. and Ikura,M. (1995) Solution structure of the epithelial cadherin domain responsible for selective cell adhesion. *Science*, **267**, 386–389.
Ozawa,M. and Kemler,R. (1990) Correct proteolytic cleavage is required for the cell adhesive function of uvomorulin. *J. Cell Biol.*, **111**, 1645–1650.
Ozawa,M., Engel,J. and Kemler,R. (1990) Single amino acid substitutions in one Ca^{2+} binding site of uvomorulin abolishes the adhesive function. *Cell*, **63**, 1033–1038.
Phillipsen,A. (1998) DINO, a visualization system for structural data. http://www.bioz.unibas.ch/~xray/dino
Pokutta,S., Herrenknecht,K., Kemler,R. and Engel,J. (1994) Conformational changes of the recombinant extracellular domain of E-cadherin upon calcium binding. *Eur. J. Biochem.*, **223**, 1019–1026.
Ranscht,B. (1994) Cadherins and catenins: interactions and functions in embryonic development. *Curr. Opin. Cell Biol.*, **6**, 740–746.
Shapiro,L. *et al*. (1995) Structural basis of cell–cell adhesion by cadherins. *Nature*, **374**, 327–337.
Takeda,H., Nagafuchi,A., Shimoyama,Y. and Hirohashi,S. (1999) Dimeric E-cadherin functions as a fundamental unit at the cell–cell adhesive interface. *Nature Struct. Biol.*, in press.
Takeichi,M. (1990) Cadherins: a molecular family important in selective cell–cell adhesion. *Annu. Rev. Biochem.*, **59**, 237–252.
Takeichi,M. (1991) Cadherin cell adhesion receptors as a morphogenetic regulator. *Science*, **251**, 1451–1455.
Tamura,K., Shan,W.-S., Hendrickson,W.A., Colman,D.R. and Shapiro,L. (1998) Structure–function analysis of cell adhesion by neural (N-) cadherin. *Neuron*, **20**, 1153–1163.
Tang,L., Hung,C.P. and Schuman,E.M. (1998) A role for the cadherin family of cell adhesion molecules in hippocampal long-term potentiation. *Neuron*, **20**, 1165–1175.
Tomschy,A., Fauser,C., Landwehr,R. and Engel,J. (1996) Homophilic adhesion of E-cadherin occurs by a co-operative two-step interaction of N-terminal domains. *EMBO J.*, **15**, 3507–3514.
Turk,D. (1988) Development and usage of a molecular graphics program. PhD thesis, University of Ljubljana, Slovenia.
Wagner,G. (1995) E-cadherin: a distant member of the immunoglobulin superfamily. *Science*, **267**, 342.
Yap,A.S., Brieher,W.M., Pruschy,M. and Gumbiner,B.M. (1997) Lateral clustering of the adhesive ectodomain: a fundamental determinant of cadherin function. *Curr. Biol.*, **7**, 308–315.
Yap,A.S., Niessen,C.M. and Gumbiner,B.M. (1998) The juxtamembrane region of the cadherin cytoplasmic tail supports lateral clustering, adhesive strengthening and interaction with p120 (ctn). *J. Cell Biol.*, **141**, 779–789.

Received December 4, 1998; revised and accepted February 2, 1999